Bull. Chem. Soc. Ethiop. **2026**, 40(3), 641-654.
DOI: https://dx.doi.org/10.4314/bcse.v40i3.11
© 2025 Chemical Society of Ethiopia and The Authors
ISSN 1011-3924
Printed in Ethiopia
Online ISSN 1726-801X

SYNTHESIS OF COBALT OXIDE NANOPARTICLES USING OKRA (*ABELMOSCHUS ESCULENTUS*) FRUIT EXTRACT: ANTIBACTERIAL EFFICACY FOR TEXTILE APPLICATIONS

Ehab S. Gad[1], Medhat E. Owda[2*], Ebtsam K. Alenezy[1], Ahmed M. Saeed[2], Abdelrahman K. Khalaf[2], Salem S. Salem[3]

[1]Department of Chemistry, College of Science, Jouf University, Sakaka 72341, Saudi Arabia
[2]Department of Chemistry, Faculty of Science (boys), Al-Azhar University, 11884 Nasr City, Cairo, Egypt
[3]Botany and Microbiology Department, Faculty of Science, Al-Azhar University, Nasr City, Cairo, 11884, Egypt

(Received August 14, 2025; Revised September 29, 2025; Accepted November 25, 2025)

ABSTRACT. The increasing threat of microbial infections on surfaces has created a critical demand for effective antimicrobial textiles. This research addresses this need by fabricating a nanocomposite textile with antimicrobial functionality, incorporating cobalt oxide nanoparticles (Co_3O_4 NPs) synthesized through an eco-friendly and cost-efficient method utilizing okra fruit (OF) extract. In the initial phase, the produced cobalt oxide nanoparticles underwent characterization using appropriate analytical techniques such as scanning electron microscopy-energy dispersive x-ray spectroscopy (SEM-EDX), Fourier transform infrared spectroscopy (FTIR), x-ray diffraction (XRD), transmission electron microscopy (TEM), Zeta potential and dynamic light scattering (DLS) technique. The results showed that a homogeneous shape with a rod-like structure in the diameter range from 4 to 11 nm. spectroscopy revealed a distinct absorption band at 551 cm^{-1}, which corresponds to the stretching vibrations of the cobalt–oxygen (Co–O) bond. OF-Co_3O_4 nanoparticles (NPs), at 200 µL, exhibited notable antibacterial activity, forming inhibition zones measuring 27 mm against *S. aureus* and 24 mm against *E. coli*. Following antimicrobial assessment, cotton fabrics were impregnated with an OF-Co_3O_4 NP solution at a concentration of 1000 µg/mL. At this dosage, the treated fabrics demonstrated strong antibacterial properties, reducing bacterial growth by 81.8% for *S. aureus* and 76.5% for *E. coli*.

KEY WORDS: Cobalt oxide nanoparticles, Phyto-synthesis, Antibacterial, Medical textiles

INTRODUCTION

Nanoparticles (NPs) have become a central focus of scientific research in recent years due to their remarkable traits, like surface plasmon resonance, unparalleled redox reversibility, and distinctive optical characteristics [1, 2]. These properties have driven NPs utilization across multiple domains, including gene therapy, drug delivery systems, and biotechnological innovations. The widespread industrial adoption of metal and metal-oxide nanoparticles directly correlates with their exceptional chemical and physical properties [3-5]. Importantly, these functional attributes depend heavily on nanoparticle morphology, dimensions, and elemental composition, making precise control over these parameters essential [6-7]. This nanoscale precision lies at the heart of nanotechnology, a fast-growing scientific discipline achieving global recognition. The field's capacity to engineer innovative materials stems from nanomaterials' reduced size and enhanced surface-area-to-volume ratios. These features have enabled groundbreaking applications in diverse sectors such as biomedical engineering, catalytic processes, renewable energy systems, environmental cleanup, and advanced water purification technologies [5, 8, 9].

Notably, nanoscale substances have attracted considerable interest in their antibacterial capabilities. Laboratory studies confirm that specific antimicrobial nanoparticles and their

*Corresponding author. E-mail: medhatowda@azhar.edu.eg
This work is licensed under the Creative Commons Attribution 4.0 International License

delivery systems effectively combat infectious diseases, including antibiotic-resistant strains [10]. Intensive research efforts have focused on analyzing the structural and reactive properties of metallic substances like magnesium oxide (MgO), silver (Ag), zinc oxide (ZnO), and copper oxide (CuO) for developing next-generation antibacterial agents [10-13].

Numerous methodologies have been developed for the synthesis of nanoparticles (NPs), including precipitation, sol-gel processing, wet chemical approaches, microwave-assisted synthesis, electrochemical techniques, hydrothermal treatment, and reverse micelle systems [14-17]. Despite their effectiveness, these conventional physical and chemical strategies often entail high costs and the use of hazardous chemicals, raising both economic and environmental concerns. As a result, there is increasing interest in adopting green chemistry approaches for CoNP production, especially those that utilize plant-based materials. Plant extracts are particularly attractive for this purpose because they contain various bioactive molecules, including polyphenols, flavonoids, and glycosides that function as natural reducing agents, facilitating the transformation of metal ions into nanoparticles [18-19]. For instance, researchers have successfully synthesized CuO NPs using Calotropis procera latex [20] and have also employed pomegranate (Punica granatum) peel extract to convert cobalt nitrate hexahydrate into nanoparticles [21]. The appeal of using fruit extracts lies in both their rich phytochemical content and the widespread availability of fruits, making them a sustainable resource for nanoparticle fabrication [22]. Compounds such as antioxidants, flavonoids, catechins, anthocyanidins, isothiocyanates, isoflavones, polyphenols, and carotenoids, classified as primary and secondary metabolites play a pivotal role in the reduction process [23]. Notably, pomegranate peel waste has been repurposed for the synthesis of various metal oxide nanoparticles [24], and fresh fruit extracts have enabled the development of diverse hybrid nanostructures, including nanowires, nanospheres, nanotubes, and nanocomposites [25].

Nanomaterials enhance antimicrobial properties in textiles through their high surface area-to-volume ratio and reactivity, allowing effective interaction with microbes to reduce hospital-acquired infections (HAIs) without degrading fabric quality. Metal oxide nanoparticles like silver (Ag), zinc oxide (ZnO), and titanium dioxide (TiO_2) provide durable protection via methods such as polymer binders or sonochemical deposition, maintaining efficacy after multiple washes for healthcare applications [26].

This research reports the eco-friendly biosynthesis of Co_3O_4 NPs employing an aqueous extract derived from okra fruit. The synthesized nanoparticles were comprehensively characterized using a range of analytical techniques, including FTIR, XRD, SEM and TEM, while EDAX was used to determine the elemental composition. In conjunction with the synthesis and characterization processes, the antibacterial efficacy of the Co_3O_4 NPs was evaluated. Prior to their application on textile substrates, the minimum inhibitory concentration (MIC) of the biosynthesized nanoparticles was determined. Subsequently, the antimicrobial performance of the treated textiles was assessed following the incorporation of Co_3O_4 NPs at a concentration of 1000 mg/L.

EXPERIMENTAL

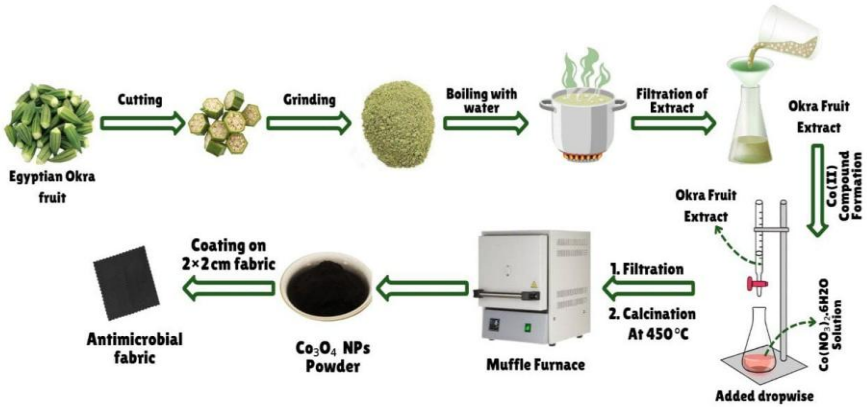
Materials and methods

Cobalt nitrate hexahydrate was purchased from Sigma-Aldrich, USA. Okra fruit was collected from the local market in Egypt.

Green synthesis of Co_3O_4 NPs

To synthesize cobalt-oxide nanoparticles (Co_3O_4 NPs), an aqueous extract of *Abelmoschus esculentus* fruit, prepared by heating washed and cut okra in distilled water followed by filtration,

is slowly added dropwise to a 1M cobalt-nitrate hexahydrate $Co(NO_3)_2.6H_2O$ solution under continuous stirring at room temperature. The resulting mixture is then heated to 70°C and maintained for 3 h. The formed nanoparticles are separated by centrifugation, washed three times with distilled water, and finally calcined at 450°C for 3 hours to obtain pure Co_3O_4 NPs, which are then stored in a dry, airtight container. Eventually, the Co_3O_4 NPs product was gathered and put through additional testing (Scheme 1).



Scheme 1. Schematic illustration of bio-synthesized OF-Co_3O_4 NPs.

Characterization of OF-Co_3O_4 NPs

The prepared samples were characterized using advanced analytical approaches. Surface and structural morphology were examined via High Resolution SEM (FEI Quanta FEG 250) operating at accelerating voltages ranging from 200 V to 30 kV, while functional groups were identified using ATR-FTIR (THERMO NICLOT 50) equipped with a built-in diamond ATR module offering a spectral range of 5000-80 cm^{-1}, a resolution better than 0.09 cm^{-1}. Crystalline structure analysis was conducted through XRD (Bruker D2 Phaser, 2nd generation) employing a Cu Kα radiation source at 30 kV and 10 mA, with a theta/theta goniometer configuration, a 2θ measurement range from -5° to 80°, and particle size distribution along with zeta-potential were measured using Dynamic-Light Scattering (ZetaSizer-Nano Series (HT), Malvern-Instruments, UK) utilizing a 633 nm He-Ne laser to determine hydrodynamic diameters from 0.3 nm to 10 μm and zeta potentials in the range of ± 500 mV.

Evaluation of antibacterial properties of OF-Co_3O_4 NPs

The antibacterial performance of the synthesized OF-Co_3O_4 NPs was assessed using the agar well-diffusion technique to establish the minimum inhibitory concentration (MIC) [27]. Both Gram-positive (Staphylococcus aureus -ATCC6538) and Gram-negative (Escherichia coli -ATCC8739) bacterial strains were utilized as test organisms. Mueller-Hinton agar served as the growth medium. After 24 hours, a microbial suspension was prepared and adjusted to a turbidity of 0.5 McFarland standard. This suspension was then added to a sterilized (autoclaved) growth medium. The inoculated medium was evenly poured into sterile Petri dishes and allowed to solidify. Once set, 8 mm wells were aseptically created in the agar using a sterile cork borer. A range of OF-Co_3O_4 NPs concentrations (10,000, 5,000, 2,500, 1,250, 625, and 312.5 μg/mL) was prepared in colloidal form. Each concentration was introduced into separate wells on the agar plates. The plates were initially placed in refrigeration for one hour to allow OF-Co_3O_4 NPs diffusion, followed by incubation at 37 °C for 24 hours. After the incubation period, the diameters of the

inhibition zones were measured in millimeters, and all tests were conducted in triplicate to ensure accuracy.

Fabric functionalization with OF-Co_3O_4 NPs

Prior to treatment, fabric samples (15 × 30 cm) were thoroughly cleaned with water and dried. The OF-Co_3O_4 NPs solution was applied to the fabric using a dip-coating technique at the MIC-derived concentration deemed safe. Each fabric was soaked in the solution for five minutes and then passed through a laboratory padder to achieve 100% wet pickup under controlled pressure. After treatment, the fabrics were dried at 80 °C for five minutes and then cured at 150 °C for two minutes. The experiment included the following treatment groups: Controls: negative control: Trypticase Soy Broth (TSB) without any bacterial inoculation. Positive control: Untreated fabric placed in TSB inoculated with bacteria. Blank: Untreated fabric placed in sterile TSB. Experimental group: Fabric samples coated with OF-Co_3O_4 NPs.

Surface morphology via scanning electron microscopy (SEM)

The surface characteristics of both treated and untreated cotton fabrics were analyzed using a JEOL JSM-5400 SEM. OF-Co_3O_4 NPs were mounted on stubs and coated with a thin layer of gold using a sputter coater prior to imaging.

Assessment of antibacterial efficiency in treated fabrics by OF-Co_3O_4 NPs

The antimicrobial activity of the nanoparticle-treated fabrics was tested against Staphylococcus aureus (ATCC 6538) and Escherichia coli (ATCC 8739). Fabric samples (1 cm^2) were placed into 5 mL of TSB medium, each containing 100 µL of bacterial suspension adjusted to an optical density (OD) of 1.0 at 600 nm. After 24 hours of incubation, bacterial growth was evaluated by measuring the optical density at 630 nm [28]. Since OD values correlate with bacterial concentration, the bacteriostatic efficiency of the fabric treatment was determined using the formula below:

Bacterial reduction (%) = [OD control - OD treated /OD control] ×100

where: OD (control) refers to the optical density of the positive control; OD (treated) refers to the optical density of the treated sample. This calculation provided a quantitative measure of bacterial inhibition as a result of the OF-Co_3O_4 NP treatment on textile substrates.

RESULTS AND DISCUSSION

Morphological analysis

The morphological characteristics of Co_3O_4 nanoparticles were examined, with the corresponding SEM micrograph presented in Figure 1. The image reveals a uniform particle shape and a narrow size distribution across the sample. Particle aggregation observed in the green-synthesized nanoparticles is attributed to the specific properties of the plant extract and the nature of its phytochemical constituents [25]. The incorporation of okra fruit extract was found to suppress nucleation while enhancing the growth rate, thereby promoting the development of larger aggregates with irregular, rock-like morphologies [29]. Biological compounds with surface functionalities such as carboxyl, hydroxyl, amino, and thio groups can passivate nanoparticle surfaces. However, these same groups can also form intermolecular hydrogen bonds, potentially causing particle agglomeration [30]. EDX with mapping was employed to determine the elemental

composition of the synthesized Co_3O_4-NPs nanoparticles (NPs), as depicted in Figure 1 B-E. The prominent peaks in the spectrum confirm the presence of cobalt (Co) and oxygen (O), the primary constituents of the synthesized NPs, along with a carbon (C) peak. Quantitative analysis of the EDX data revealed a composition of approximately 59 wt% cobalt and 26.4 wt% oxygen, consistent with the expected stoichiometry of cobalt oxide Co_3O_4-NPs. The presence of 13.8 wt% carbon may be attributed to residual organic matter from the plant extract. The EDX spectrum exhibits distinct peaks in the 0-1 keV and 6-8 keV regions, characteristic of crystalline Co_3O_4-NPs nanoparticles. The simultaneous detection of cobalt and oxygen unequivocally confirms the formation of cobalt oxide in the synthesized material [31].

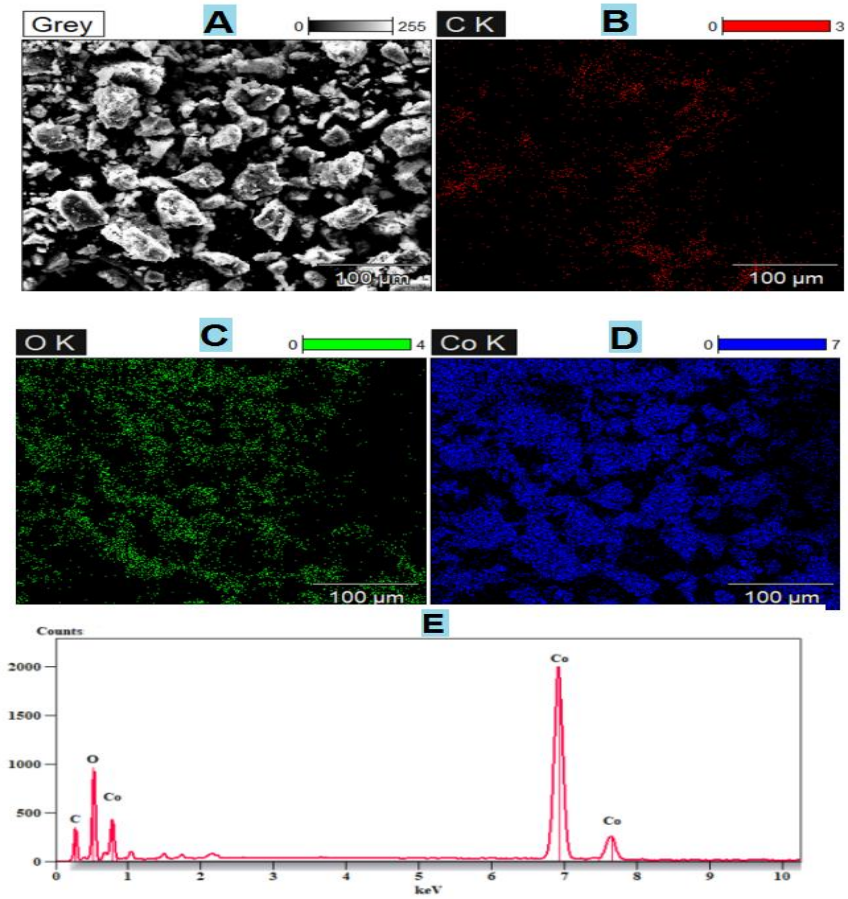


Figure 1. SEM image (A), Elemental mapping (B-D), and EDX (E) of Co_3O_4-NPs.

FTIR and XRD analysis

The surface chemistry of the synthesized okra fruit-mediated OF-Co_3O_4 NPs was analyzed using FTIR spectroscopy. As illustrated in Figure 2A, the spectrum displays multiple absorption bands corresponding to various functional groups involved in nanoparticle formation. Prominent peaks were observed at 3345, 2927, 1643, 1353, 1052, 655, and 550 cm^{-1}. The broad absorption at 3345 cm^{-1} is indicative of hydroxyl group presence, while the peak at 2927 cm^{-1} is attributed to C–H

stretching vibrations of alkanes [32]. The band at 1643 cm^{-1} corresponds to carbonyl (C=O) groups [25], and the signal at 1531 cm^{-1} is associated with C=C stretching, reflecting the aromatic skeletal framework of the extract. Additionally, the peak at 1353 cm^{-1} signifies C–C stretching within aromatic compounds, and the absorption at 1052 cm^{-1} is linked to C–O stretching vibrations [32].

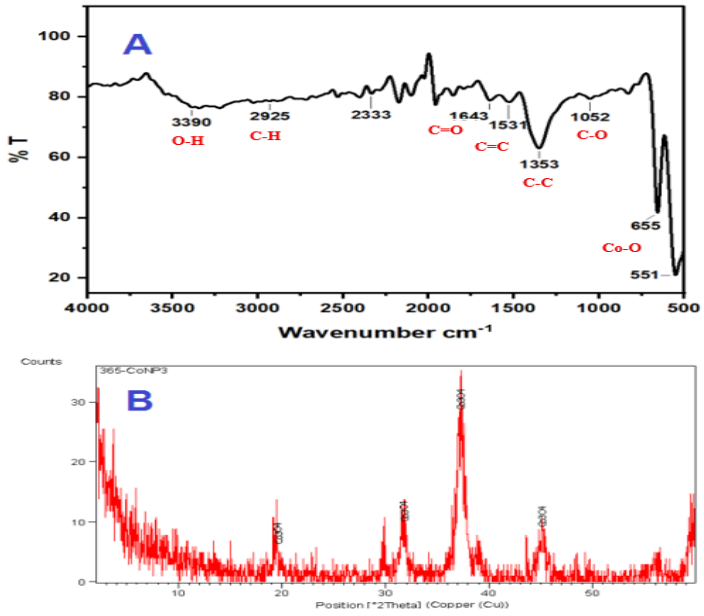


Figure 2. FTIR (A) and XRD(B) of OF- Co_3O_4 NPs.

The bands near 655 cm^{-1} and 550 cm^{-1} are characteristic of Co–O vibrations, confirming the transformation of cobalt hydroxide into cobalt oxide and the thermal decomposition of organic constituents from the plant extract [33]. Further structural analysis was performed using XRD, with the pattern of Co_3O_4 nanoparticles post-calcination at 450 °C presented in Figure 2B. The diffraction peaks observed at 2θ values of 19.27°, 31.52°, 37.25°, 45.02° and 59.62° correspond to the (111), (220), (311), (400) and (511) crystal planes, respectively, and are consistent with the face-centered cubic (FCC) structure of Co_3O_4 nanoparticles [7]. Based on the Scherrer equation, the average crystallite size of the OF-Co_3O_4 NPs was estimated to be approximately 10.7 nm. The data further suggests that multiple crystallites have aggregated to form the final nanoparticle structure.

TEM, zeta potential, and DLS analysis

TEM imaging revealed cobalt oxide nanoparticles displaying diverse morphologies (Figure 3A), with a notable prevalence of elongated, rod-shaped structures alongside ovoid forms. Dimensional analysis of the nanoparticles indicated sizes ranging from 4 to 11 nm. Despite the heterogeneity in individual particle diameters, the majority resided within the nanoscale, yielding an average particle size of 9.70 nm according to the histogram (Figure 3D). This average is consistent with the nanoscale nature of the material as suggested by XRD data. Furthermore, the nanoparticles exhibited a marked tendency to self-assemble into irregular clusters. The zeta potential of the synthesized OF-Co_3O_4 nanoparticles was measured to be −36.2 mV (Figure 3B), indicating a

negatively charged surface. This negative surface charge generates electrostatic repulsion among particles, thereby promoting colloidal stability and preventing aggregation [34]. Typically, nanoparticles with zeta potential values exceeding +25 mV or below −25 mV are considered to possess significant stability due to strong repulsive forces. In this case, the negative charge is attributed to the capping agents derived from the plant extract, which play a crucial role in stabilizing the nanoparticles [35]. Thus, greater surface charge magnitude correlates with enhanced stability.

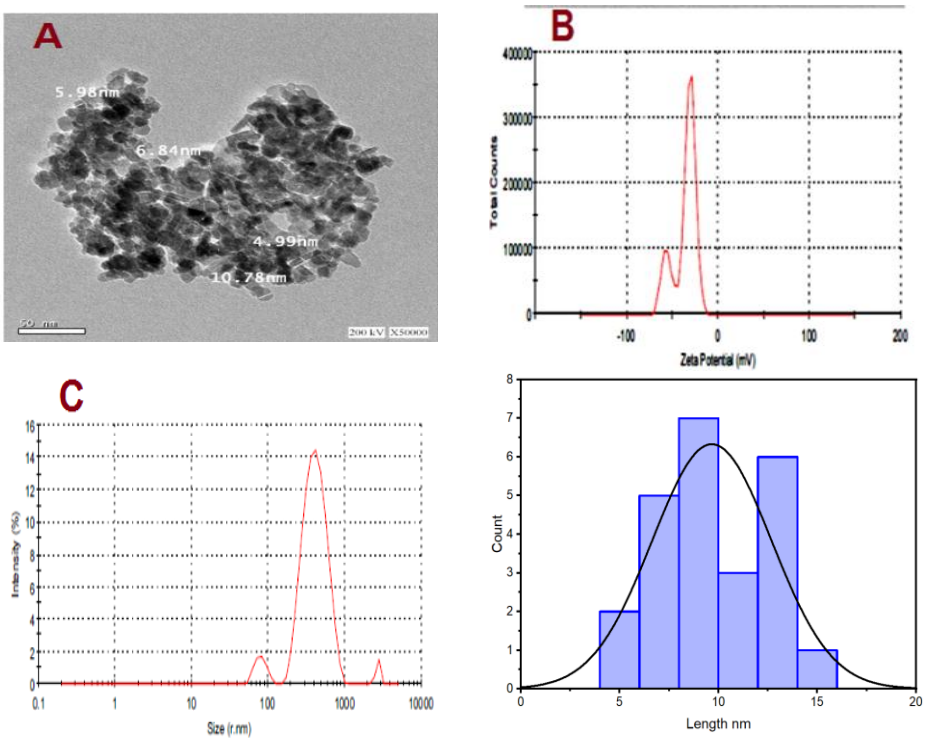


Figure 3. TEM (A) Zeta potential (B), size distribution (C) and histogram (D) of OF- Co_3O_4 NPs.

To further characterize the nanoparticles, DLS analysis was performed (Figure 3C), revealing an average hydrodynamic diameter of approximately 376 nm and a polydispersity index (PDI) of 0.334. Since the PDI value is below 0.5, the nanoparticle dispersion is considered monodisperse. However, some degree of agglomeration may occur due to intermolecular hydrogen bonding among the bioactive compounds present in the plant extract [36]. Comparative literature (Bibi et al., 2017), reports the synthesis of uniform, spherical cobalt oxide nanoparticles with diameters below 80 nm using Punica granatum peel extract. In contrast, scanning electron microscopy (SEM) analysis of the OF-Co_3O_4 nanoparticles (Figure 1) shows aggregated structures with varying diameters. The observed discrepancy between particle sizes obtained from DLS and those visualized via transmission electron microscopy (TEM) can be attributed to the angle-dependent nature of light scattering in DLS measurements [21] .

Antibacterial activity of OF- Co_3O_4 NPs with MIC

The antimicrobial activity of OF-Co_3O_4 NPs was analyzed by the agar well diffusion method at 10000 µg/mL of cobalt oxide nanoparticles. The OF-Co_3O_4 NPs exhibited good antimicrobial activity against two pathogenic bacteria. The results, represented graphically in Figure 4, revealed that the two tested microorganisms were inhibited by OF- Co_3O_4 NPs.

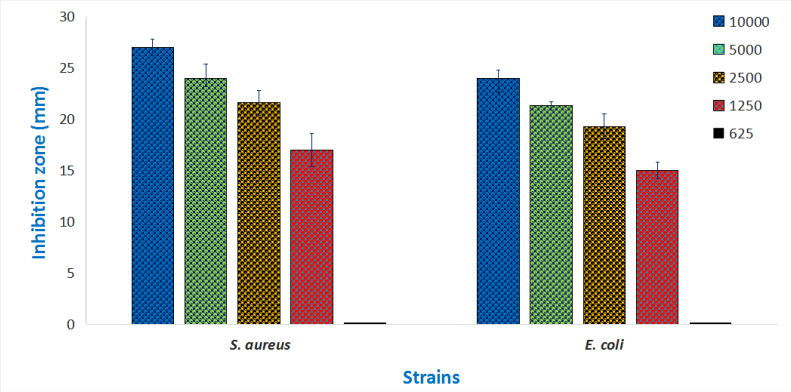


Figure 4. Antibacterial activity and MIC determination of OF-Co_3O_4 NPs at varying concentrations.

The inhibition zone produced by OF-Co_3O_4 NPs was 27 and 24 mm for *S. aureus* and *E. coli*, respectively. The observed inhibition zones are consistent with previous studies that have reported the antimicrobial efficacy of cobalt oxide nanoparticles. The diameter of the inhibitory zone formed by OF- Co_3O_4 NPs was correlated to its concentration, so that the MIC for each bacterial strain must be determined. To achieve this goal, different concentrations of OF- Co_3O_4 NPs were used (10,000, 5,000, 2,500, 1,250, 625, and 312.5 µg/mL). Data in Figure (4) revealed that 1250 µg/mL was the minimum concentration of OF-Co_3O_4 NPs having inhibitory action against *S. aureus and E. coli.* The results showed a concentration-dependent antibacterial response, with higher concentrations yielding larger zones of inhibition. The lowest concentration that exhibited a visible inhibitory effect against both bacterial strains was identified as the MIC. OF-Co_3O_4 NPs were particularly effective against S. aureus, indicating a stronger activity against Gram-positive bacteria, although significant inhibition was also observed against *E. coli.* These findings suggest that OF-Co_3O_4 NPs possess broad-spectrum antibacterial properties and can be considered effective antimicrobial agents at relatively low concentrations. These observations are in good agreement with earlier work on Co_3O_4 nanoparticles. For instance, synthesized Co_3O_4 NPs demonstrated dose-dependent activity against *S. aureus* and *E. coli*, with inhibition zone diameters ranging from approximately 22 mm up to 45 mm at different doses from Co_3O_4 NPs [38]. Another study found that Co/Co_3O_4 nanocomposites displayed MICs of around 500 µg/mL for both *S. aureus* and *E. coli*, along with MBCs between 1000–2000 µg/mL [39-40]. For instance, Akhter et al., [41], found inhibition zones of approximately 23 mm for *S. aureus* and 28 mm for *E. coli* at nearly Co_3O_4NPs concentrations, suggesting that the antimicrobial activity in this study is comparable or slightly enhanced. Other studies, Girma et al., [42] have also confirmed that Gram-positive bacteria such as *S. aureus* tend to be more susceptible to metal oxide nanoparticles than Gram-negative bacteria like *E. coli*, likely due to differences in cell wall structure.

Integration of Biosynthesized OF-Co_3O_4 Nanoparticles into Cotton Fabric

Due to their notable antibacterial properties, the biosynthesized OF-Co_3O_4 NPs were incorporated into cotton fabrics for potential use in antimicrobial textiles. The application method followed protocols established in our prior research. A colloidal suspension of OF-Co_3O_4 NPs was prepared by dispersing the nanoparticles in distilled water to achieve a final concentration of 1000 µg/mL. The presence and uniform distribution of OF-Co_3O_4 NPs on the fabric surface were confirmed through SEM, coupled with EDX, as illustrated in Figure 5A–C. SEM imaging of the treated fabric (Figure 5B) revealed a consistent and homogeneous layer of nanoparticle deposition, in contrast to the untreated control fabric (Figure. 5A), which displayed a smooth and clean surface.

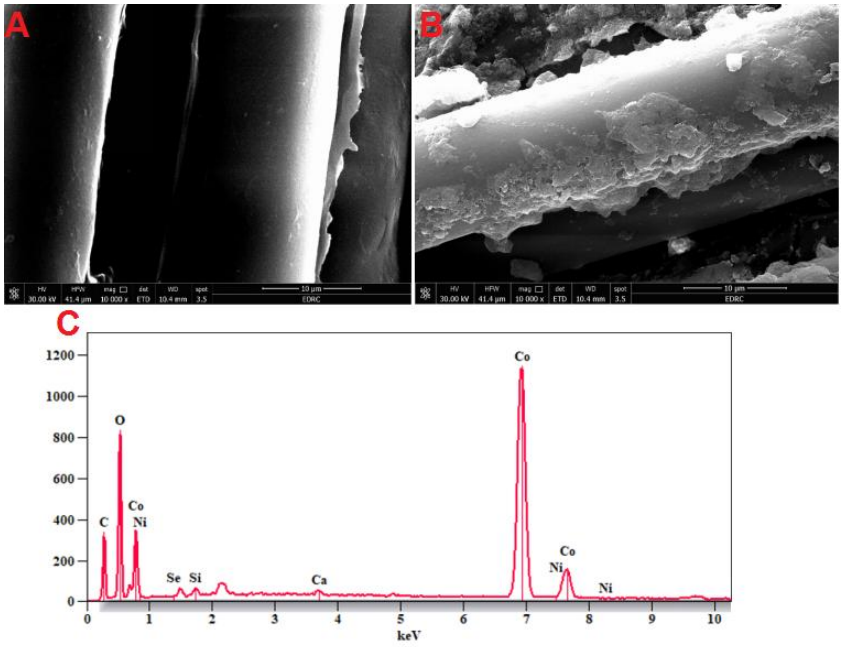


Figure 5. (A) Untreated cotton-fabric SEM image, (B) Treated cotton-fabric with OF-Co_3O_4 nanoparticles SEM image, and (C) EDX spectrum of cotton fabric treated with Co_3O_4 NPs.

Furthermore, EDX analysis was employed to determine the elemental composition of the coated fabrics. The EDX spectrum (Figure 5C) indicated that cobalt, a constituent of the cobalt oxide nanoparticles, accounted for approximately 26.1% of the total elemental content detected in the treated sample, thereby confirming successful OF-Co_3O_4 NPs incorporation. These findings are consistent with earlier reports involving the application of metal oxide nanoparticles to textile substrates. For instance, Ali et al., [43] demonstrated successful coating of cotton fabrics with Co_3O_4 nanoparticles synthesized via a chemical precipitation method, resulting in similar surface coverage and antibacterial properties. Investigations on CuO and ZnO nanoparticles have also shown comparable levels of adhesion and surface morphological alterations following loading on cotton textiles [27]. These results confirm the successful integration of OF-Co_3O_4 NPs into cotton fibers, enhancing the fabric's functional properties and establishing its potential for use in antimicrobial textile applications.

The antimicrobial effectiveness of cotton fabrics treated with OF-Co_3O_4 NPs was investigated by measuring the percentage reduction of pathogenic bacteria. As presented in Figure 6, the

treated fabrics demonstrated significant antibacterial activity against both tested strains. Specifically, the bacterial reduction reached 81.8% for *S. aureus* and 76.5% for *E. coli*. These findings highlight the enhanced antimicrobial functionality imparted by the OF-Co_3O_4 NPs, which were effectively anchored onto the cotton fibers, enabling the fabric to inhibit bacterial growth. In comparative treatments using Cu-O, Zn-O, Co-O, Fe-O, and Mn-O nanoparticles, all fabrics showed high antibacterial efficiency, with a variety of bacterial inactivation [28,44]. These results confirm the successful integration of OF-Co_3O_4 NPs into cotton fibers, enhancing the fabric's functional properties and establishing its potential for use in antimicrobial textile applications.

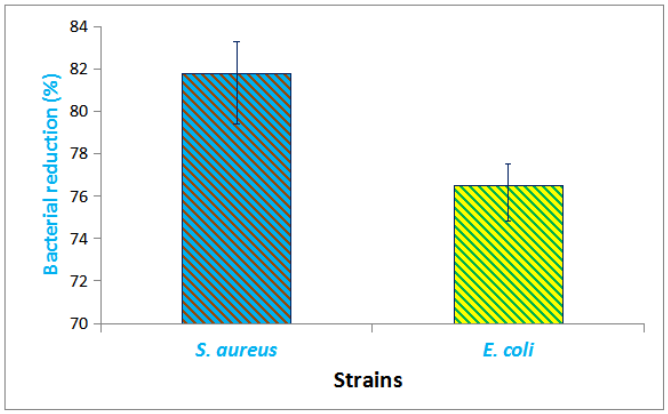


Figure 6. Antibacterial Efficiency of OF-Co_3O_4 NP-Treated Fabrics Assessed using bacterial-reduction (%).

CONCLUSIONS

Co_3O_4 nanoparticles were successfully synthesized via a green method using okra fruit extract, which served as both a reducing and stabilizing agent. This solvent-free approach aligns with sustainable chemistry principles and eliminates the need for external catalysts or templates. The presence of biomolecules such as phenols and tannins facilitated the formation of rod-shaped nanoparticles with sizes ranging from 4 to 11 nm. Zeta potential analysis revealed a strong negative surface charge, indicating good colloidal stability, while particle size distribution confirmed uniformity and minimal aggregation. These results demonstrate the effectiveness of plant-mediated synthesis in producing stable, nanoscale materials with potential applications in the coating of fabric. Regarding the antimicrobial outcomes, the textiles were treated with 1000µg/mL of OF-Co_3O_4 NPs, which demonstrated good antimicrobial effects against pathogens.

ACKNOWLEDGMENTS

The authors extend their appreciation to the Deanship of Graduate Studies and Scientific Research at Jouf University for funding this work through research grant No. (DGSSR-2024-02-01259).

Data availability

All data generated or analyzed during this study are included in this published article.

Declaration of competing interest

This paper was written by the authors without any personal, financial, or non-financial conflicts of interest.

Funding

This work was funded by the Deanship of Graduate Studies and Scientific Research at Jouf University under grant No. (DGSSR-2024-02-01259).

Authors' contributions

Ehab S. Gad: Methodology, Writing - review & editing Data curation. Medhat E. Owda: Conceptualization, Formal analysis, Investigation, Methodology, Writing - review & editing Data curation. Ebtsam K. Alenezy: Methodology, Writing - review & editing Data curation. Ahmed M. Saeed: Conceptualization, Formal analysis, Investigation, Methodology, Writing - review & editing, Data curation. Abdelrahman. K. Khalaf: Methodology, Writing - review & editing Data curation. Salem S. Salem: Conceptualization, Formal analysis, Investigation, Methodology, Writing - review & editing, Data curation.

REFERENCES

1. Ajarem, J.S.; Maodaa, S.N.; Allam, A.A.; Taher, M.M.; Khalaf, M. Benign synthesis of cobalt oxide nanoparticles containing red algae extract: Antioxidant, antimicrobial, anticancer, and anticoagulant activity. *J. Clust. Sci.* **2022**, 33, 717-728.
2. Adekunle, A.S.; Oyekunle, J.A.O.; Durosinmi, L.M.; Oluwafemi, O.S.; Olayanju, D.S.; Akinola, A.S.; Obisesan, O.R.; Akinyele, O.F.; Ajayeoba, T.A. Potential of cobalt and cobalt oxide nanoparticles as nanocatalyst towards dyes degradation in wastewater. *Nano-Struct. Nano-Objects* **2020**, 21, 100405.
3. Kgosiemang, I.K.; Lefojane, R.; Direko, P.; Madlanga, Z.; Mashele, S.; Sekhoacha, M. Green synthesis of magnesium and cobalt oxide nanoparticles using *Euphorbia tirucalli*: Characterization and potential application for breast cancer inhibition. *Inorg. Nano-Met. Chem.* **2020**, 50, 1070-1080.
4. Pagar, T.; Ghotekar, S.; Pagar, K.; Pansambal, S.; Oza, R. A review on bio-synthesized Co_3O_4 nanoparticles using plant extracts and their diverse applications. *J. Chem. Rev.* **2019**, 1, 260-270.
5. Salem, S. S. A mini review on green nanotechnology and its development in biological effects. *Arch. Microbiol.* **2023**, 205, 128.
6. Salem, S.S.; Fouda, A. Green synthesis of metallic nanoparticles and their prospective biotechnological applications: An overview. *Biol. Trace. Elem. Res.* **2021**, 199, 344-370.
7. Mohandes, A.; Aghamaali, M. R.; Sabouri, Z.; Darroudi, M. Biosynthesis of cobalt oxide nanoparticles (Co_3O_4-NPs) using *Caccinia macranthera* extract and evaluation of their cytotoxicity and photocatalytic activity. *Mater. Sci. Eng B-Adv.* **2023**, 297, 116782.
8. Dahl, J.A.; Maddux, B. L.S.; Hutchison, J.E. Toward greener nanosynthesis. *Chem. Rev.* **2007**, 107, 2228-2269.
9. Ramalakshmi, C.; Suresh, S.; Murugan, A.M.; Alyami, N.M.; Aljawdah, HM.; Alharbi, S.A.; Mariselvam, R. Green synthesis of copper nanoparticles from Terminalia arjuna (L.) bark extract: Characterization and potential for mercury degradation. *Bull. Chem. Soc. Ethiop*. **2024**, 38, 1703-1713.

10. Fatiqin, A.; Amrulloh, H.; Simanjuntak, W. Green synthesis of MgO nanoparticles using Moringa oleifera leaf aqueous extract for antibacterial activity. *Bull. Chem. Soc. Ethiop*. **2021**, 35, 161-170.
11. Gatasheh, M.K. Synthesis and characterization of silver nanoparticles from Cocos nucifera L. male flowers: An investigation into their potent antibacterial and anticancer efficacy. *Bull. Chem. Soc. Ethiop*, **2024**, 38, 715-724.
12. Gad, E.S.; Salem, S.S.; Selim, S.; Almuhayawi, M.S.; Alruhaili, M.H.; Al Jaouni, S.K.; Saddiq, A.A.; Owda, M.E. A comprehensive study on characterization of biosynthesized copper-oxide nanoparticles, their capabilities as anticancer and antibacterial agents, and predicting optimal docking poses into the cavity of *S. Aureus* DHFR. *PLoS One* **2025**, 20 , e0319791.
13. Selim, S.; Salem, S.S.; Owda, M.E.; Almuhayawi, M.S.; Gattan, H.S.; Alruhaili, M.H.; Saddiq, A.A.; Hussein, S.; Al-Sanea, M.M.; Al Jaouni, S.K. biosynthesized zinc oxide nanoparticles: Multifunctional potential applications in anticancer, antibacterial, and B. subtilis DNA gyrase docking. *Green Process Synth*. **2025**, 14, 20240218.
14. Mittal, A.K.; Chisti, Y.; Banerjee, U.C. Synthesis of metallic nanoparticles using plant extracts. *Biotechnol Adv.* **2013**, 31, 346-356.
15. Kandpal, N.D.; Sah, N.; Loshali, R.; Joshi, R.; Prasad, J. Co-precipitation method of synthesis and characterization of iron oxide nanoparticles. *J. Sci. Ind. Res*. **2014**, 73, 87-90
16. Bayal, N.; Jeevanandam, P. Synthesis of TiO2− MgO mixed metal oxide nanoparticles via a sol− gel method and studies on their optical properties. *Ceram. Int.* **2014**, 40, 15463-15477.
17. Salimi, A.; Mamkhezri, H.; Hallaj, R.; Soltanian, S. Electrochemical detection of trace amount of arsenic(III) at glassy carbon electrode modified with cobalt oxide nanoparticles. *Sens. Actuators B Chem.* **2008**, 129, 246- 254.
18. Singh, J.; Dutta, T.; Kim, K.-H.; Rawat, M.; Samddar, P.; Kumar, P. 'Green' synthesis of metals and their oxide nanoparticles: applications for environmental remediation. *J. Nanobiotechnology* **2018**, 16, 1-24.
19. Basavegowda, N.; Idhayadhulla, A.; Lee, Y. R. Preparation of Au and Ag nanoparticles using artemisia annua and their in vitro antibacterial and tyrosinase inhibitory activities. *Mat. Sci. Eng. C-Mater.* **2014**, 43, 58-64.
20. Dubey, S.; Sharma, Y.C. Calotropis Procera mediated one pot green synthesis of cupric oxide nanoparticles (CuO-NPs) for adsorptive removal of Cr (VI) from aqueous solutions. *Appl. Organomet. Chem.* **2017**, 31, e3849.
21. Bibi, I.; Nazar, N.; Iqbal, M.; Kamal, S.; Nawaz, H.; Nouren, S.; Safa, Y.; Jilani, K.; Sultan, M.; Ata, S. Green and eco-friendly synthesis of cobalt-oxide nanoparticle: Characterization and photo-catalytic activity. *Adv. Powder Technol.* **2017**, 28, 2035-2043.
22. Sheng, Y.; Narayanan, M.; Basha, S.; Elfasakhany, A.; Brindhadevi, K.; Xia, C.; Pugazhendhi, A. In vitro and in vivo efficacy of green synthesized AgNPs against gram negative and gram positive bacterial pathogens. *Process Biochem.* **2022**, 112, 241-247.
23. Ajduković, M.; Stojadinović, S.; Marinović, S.; Milutinović-Nikolić, A.; Dojčinović, B.; Banković, P. Activation of oxone® with plasma deposited mixed cobalt and alumina oxide for the dye degradation. *Appl. Surf. Sci.* **2020**, 503, 144144.
24. Ali, J.A.; Ahmed, R.N.; Abdullah, A.D.; Ali, N.H.; Kalhury, A.M.; Sabir, A.N.; Khaksar Manshad, A.; Keshavarz, A.; Mohammadi, A.H. Development of a nanobiodegradable drilling fluid using *Prosopis farcta* plant and pomegranate peel powders with metal oxide nanoparticles. *ACS Omega.* **2022**, 7, 31327-31337.
25. Shanmuganathan, R.; Sathiyavimal, S.; Le, Q.H.; Al-Ansari, M.M.; Al-Humaid, L.A.; Jhanani, G.K.; Lee, J.; Barathi, S. Green synthesized cobalt oxide nanoparticles using curcuma longa for anti-oxidant, antimicrobial, dye degradation and anti-cancer property. *Environ Res.* **2023**, 236, 116747.

26. Dejene. B.K. Biosynthesized ZnO nanoparticle-functionalized fabrics for antibacterial and biocompatibility evaluations in medical applications: A critical review. *Mater. Today Chem*. **2024,** 42, 102421.
27. Shaheen, T.I.; Fouda, A.; Salem, S.S. Integration of cotton fabrics with biosynthesized CuO nanoparticles for bactericidal activity in the terms of their cytotoxicity assessment. *Ind. Eng. Chem. Res.* **2021**, 60, 1553-1563.
28. Fouda, A.; Saad, E.L.; Salem, S.S.; Shaheen, T.I. In-vitro cytotoxicity, antibacterial, and UV protection properties of the biosynthesized zinc oxide nanoparticles for medical textile applications. *Microb. Pathog.* **2018**, 125, 252-261.
29. Batool, S.; Hasan, M.; Dilshad, M.; Zafar, A.; Tariq, T.; Wu, Z.; Chen, R.; Hassan, S. G.; Munawar, T.; Iqbal, F. Green synthesis of *Cordia myxa* incubated ZnO, Fe2O3, and Co_3O_4 nanoparticle: Characterization, and their response as biological and photocatalytic agent. *Adv. Powder Technol.* **2022**, 33, 103780.
30. Mafa, P.J.; Malefane, M.E.; Idris, A.O.; Mamba, B.B.; Liu, D.; Gui, J.; Kuvarega, A.T. Cobalt oxide/copper bismuth oxide/samarium vanadate (Co_3O_4/CuBi2O4/SmVO4) dual z-scheme heterostructured photocatalyst with high charge-transfer efficiency: Enhanced carbamazepine degradation under visible light irradiation. *J. Colloid Interface Sci.* **2021**, 603, 666-684.
31. Dhas, N.A.; Raj, C.P.; Gedanken, A. Synthesis, characterization, and properties of metallic copper nanoparticles. *Chem. Mater.* **1998**, 10, 1446-1452.
32. Athawale, A. A.; Majumdar, M.; Singh, H.; Navinkiran, K. Synthesis of cobalt oxide nanoparticles/fibres in alcoholic medium using y-ray technique. *Def. Sci. J.* **2010**, 60, 507-513.
33. Dick, M.; Dal Magro, L.; Rodrigues, R.C.; de Oliveira Rios, A.; Flores, S.H. Valorization of *Opuntia monacantha* (Willd.) Haw. cladodes to obtain a mucilage with hydrocolloid features: physicochemical and functional performance. *Int. J. Biol. Macromol.* **2019**, 123, 900-909.
34. Onwudiwe, D.C.; Ravele, M.P.; Elemike, E.E. Eco-friendly synthesis, structural properties and morphology of cobalt hydroxide and cobalt oxide nanoparticles using extract of litchi chinensis. *Nano-Struct. Nano-Objects* **2020**, 23, 100470.
35. Anandalakshmi, K.; Venugobal, J.; Ramasamy, V. Characterization of silver nanoparticles by green synthesis method using pedalium murex leaf extract and their antibacterial activity. *Appl Nanosci.* **2016**, 6, 399-408.
36. Haider, M.J.; Mehdi, M.S. Study of morphology and zeta potential analyzer for the silver nanoparticles. *Int. J. Sci. Eng. Res.* **2014**, 5, 381-387.
37. Nazeruddin, G.M.; Prasad, N.R.; Prasad, S.R.; Shaikh, Y.I.; Waghmare, S.R.; Adhyapak, P. *Coriandrum sativum* Seed extract assisted in situ green synthesis of silver nanoparticle and its anti-microbial activity. *Ind. Crops Prod.* **2014**, 60, 212-216.
38. Babick, F.; Schießl, K.; Stintz, M. Characterization of pyrogenic powders with conventional particle sizing technique: I. prediction of measured size distributions. *Part. Syst. Charact.* **2012**, 29, 104-115.
39. Arsalan, N.; Kashi, E.H.; Hasan, A.; Doost, M.E.; Rasti, B.; Paray, B.A.; Nakhjiri, M.Z.; Sari, S.; Sharifi, M.; Shahpasand, K. Exploring the interaction of cobalt oxide nanoparticles with albumin, leukemia cancer cells and pathogenic bacteria by multispectroscopic, docking, cellular and antibacterial approaches. *Int. J. Nanomed.* **2020**, 15, 4607-4623.
40. Anele, A.; Obare, S.; Wei, J. Recent trends and advances of Co_3O_4 nanoparticles in environmental remediation of bacteria in wastewater. *Nanomaterials* **2022**, 12, 1129.
41. Akhter, N.; Liaquat, A.; Murtaza, F.; Yaqoob, A.; Sharif, S.; Jummah, N.; Khan, M.I.; Shanableh, A.; Voskressensky, L.G.; Luque, R. One-step phytosynthesis of Co_3O_4 nanoparticles and study of their catalytic, antioxidant, antibiofilm and antibacterial activities. *Results Chem.* **2025**, 14, 102151.

42. Girma, A.; Mebratie, G.; Mekuye, B.; Abera, B.; Bekele, T.; Alamnie, G. Antibacterial capabilities of metallic nanoparticles and influencing factors. *Nano Select* **2024**, 5, e202400049.
43. Ali, N.; Khan, A.; Asiri, A.M.; Kamal, T. Potential application of in-situ synthesized cobalt nanoparticles on chitosan-coated cotton cloth substrate as catalyst for the reduction of pollutants. *Environ. Technol. Innov.* **2021**, 23, 101675.
44. Gouda, M.; Aljaafari, A.; Al-Fayz, Y.; Boraie, W.E. Preparation and characterization of some nanometal oxides using microwave technique and their application to cotton fabrics. *J Nanomater.* **2015**, 2015, 586904.